

## Supporting Information

### Multi-Functional Biotinylated Platinum(IV)-SAHA Conjugate for Tumor-Targeted Chemotherapy

Ajay Gupta, Pijus K. Sasmal\*

School of Physical Sciences, Jawaharlal Nehru University, New Delhi 110067, India.

\*Corresponding author: [pijus@mail.jnu.ac.in](mailto:pijus@mail.jnu.ac.in)

### Table of Contents

#### 1. Instruments and Methods

- 1.1 Thin layer chromatography and column chromatography
- 1.2 NMR spectroscopy
- 1.3 Mass spectrometry
- 1.4 FT-IR spectroscopy
- 1.5 RP-HPLC analysis
- 1.6 Determination of lipophilicity

#### Supplementary Scheme and Figures

**Fig. S1** IR spectra of SAHA, **Pt(IV)-Biotin**, **SAHA-OTs**, **Pt(IV)-SAHA**, **Biotin-Pt(IV)-SAHA**

**Fig. S2-S3** <sup>1</sup>H and <sup>13</sup>C NMR spectra of **Pt(IV)-Biotin** in DMSO-d<sub>6</sub>.

**Fig. S4-S5** <sup>1</sup>H and <sup>13</sup>C NMR spectra of suberic anhydride in CDCl<sub>3</sub>.

**Fig. S6-S7** <sup>1</sup>H and <sup>13</sup>C NMR spectra of suberanilic acid in DMSO-d<sub>6</sub>.

**Fig. S8** <sup>1</sup>H spectrum of SAHA in DMSO-d<sub>6</sub>.

**Fig. S9** <sup>1</sup>H spectrum of **SAHA-OTs** in DMSO-d<sub>6</sub>.

**Fig. S10-S11** <sup>1</sup>H and <sup>13</sup>C NMR spectra of **Pt(IV)-SAHA** in DMSO-d<sub>6</sub>.

**Fig. S12-S13** <sup>1</sup>H and <sup>13</sup>C NMR spectra of **Biotin-Pt(IV)-SAHA** in DMSO-d<sub>6</sub>.

**Fig. S14** <sup>195</sup>Pt-NMR spectrum of **Pt(IV)-SAHA** in DMSO-d<sub>6</sub> at 298K.

**Fig. S15** <sup>195</sup>Pt-NMR spectrum of **Biotin-Pt(IV)-SAHA** in DMSO-d<sub>6</sub> at 298K.

**Fig. S16** ESI-HRMS spectrum of SAHA.

**Fig. S17** ESI-HRMS spectrum of **SAHA-OTs**.

**Fig. S18** ESI-HRMS spectrum of **Pt(IV)-Biotin**.

**Fig. S19** ESI-HRMS spectrum of **Pt(IV)-SAHA**.

**Fig. S20** ESI-HRMS spectrum of **Biotin-Pt(IV)-SAHA**.

**Fig. S21** HPLC chromatograms of SAHA, Pt(IV)-SAHA, and Biotin-Pt(IV)-SAHA.

**Fig. S22** HPLC chromatograms of cisplatin, oxoplatin and suberanilic acid.

**Fig. S23** Stability of SAHA in PBS and ascorbate monitored by HPLC.

**Fig. S24-S28** Plot of cell viability by MTT assay of the complexes in MCF7, A549, A2780, A2780cisR, and HEK293 cells.

**Fig. S29-S30** Drug combination studies in A2780 and A2780cisR cells.

## Supplementary References

### 1. Instruments and Methods

#### 1.1 Thin layer chromatography (TLC) and column chromatography

TLC was carried out on aluminum plates coated with silica gel mixed with fluorescent indicator. The purification of synthesized ligands and complexes were performed with silica gel (60-120 mesh) column chromatography.

#### 1.2 NMR spectroscopy

$^1\text{H}$ ,  $^{13}\text{C}$  and  $^{195}\text{Pt}$  NMR spectra were acquired on a Bruker 500 MHz spectrometer in  $\text{CDCl}_3$  or  $\text{DMSO-d}_6$  at ambient temperature with tetramethylsilane (TMS) as an internal standard. NMR standards used were as follows: ( $^1\text{H}$ -NMR)  $\text{CDCl}_3 = 7.260$  ppm;  $\text{DMSO-d}_6 = 2.50$  ppm. ( $^{13}\text{C}$ -NMR)  $\text{CDCl}_3 = 77.00$  ppm;  $\text{DMSO-d}_6 = 39.520$  ppm. All chemical shifts ( $\delta$ ) are reported in ppm relative to TMS. Spin multiplicities were reported as a singlet (s), doublet (d), triplet (t), quartet (q), doublet of doublets (dd), triplet of doublets (td), doublet of doublet of doublets (ddd), multiplet (m) and broad (br) with coupling constant ( $J$ ) reported in Hz.

#### 1.3 Mass spectrometry

Electrospray ionization high resolution mass spectra (ESI-HRMS) were obtained using a Waters make ESI-MS model synapt G2 high definition mass spectrometry. Matrix-assisted laser desorption ionization-time-of-flight (MALDI-TOF) mass spectral data were obtained using a Bruker made Autoflex TOF/TOF mass spectrometry. The spectra of all compounds were recorded using  $\alpha$ -cyano-4-hydroxycinnamic acid (CHCA) as matrix.

#### 1.4 FT-IR spectroscopy

Fourier transform-Infrared (FT-IR) spectra were measured using IR Affinity-1S (Shimadzu, Kyoto, Japan) FT-IR spectrophotometer equipped with a single reflection attenuated total reflectance (ATR) accessory. The IR spectra were recorded from  $4000$  to  $450$   $\text{cm}^{-1}$  using a resolution of  $4$   $\text{cm}^{-1}$  with 45 scans. In IR absorption spectra, the shapes and signal intensities (height) of peaks (bands) are denoted by the following abbreviations: br = broad, vs = very strong, s = strong, m = medium and w = weak.

### 1.5 RP-HPLC analysis

The purity of complexes was determined by analytical HPLC system (Thermo Scientific Dionex Ultimate 3000) equipped with UV-Vis detector using reversed-phase C18 column (Acclaim, Length 250 mm, internal dia. 4.6 mm, particle size 5  $\mu\text{m}$ , pore size 120  $\text{\AA}$ ) operating at room temperature (RT).

### 1.6 Determination of lipophilicity

The lipophilicity ( $\log P_{o/w}$ ) of the compounds (SAHA, **Pt(IV)-SAHA**, and **Biotin-Pt(IV)-SAHA**) were determined by the conventional flask-shaking method as reported in the literature.<sup>1,2</sup> Here,  $\log P_{o/w} = \log (C_o/C_w)$  is defined as the logarithmic ratio of the compound concentration in n-octanol to that in the water phase. For this, 0.5 mg of compound was taken in 3 mL of 1:1 v/v mixture of n-octanol and water, mixed vigorously for 24 h. The mixture was then kept in a stationary state for an additional 24 h to reach saturation. The n-octanol and water phases were separated, centrifuged at 3000 rpm for 10 min and the supernatant was isolated. The concentration of complexes was then determined by UV-vis spectroscopy in both the n-octanol ( $C_o$ ) and water ( $C_w$ ) phases to estimate the  $\log P_{o/w}$  values.

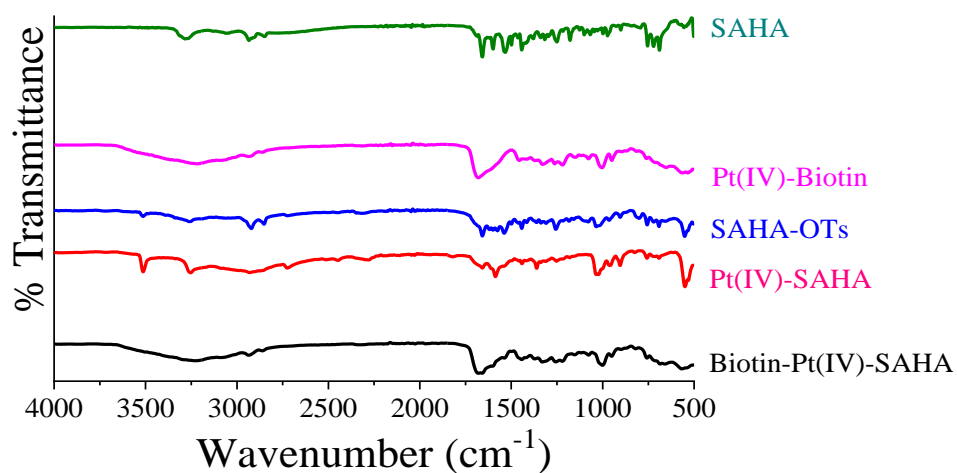


Fig. S1 IR spectra of SAHA, Pt(IV)-Biotin, SAHA-OTs, Pt(IV)-SAHA, Biotin-Pt(IV)-SAHA.

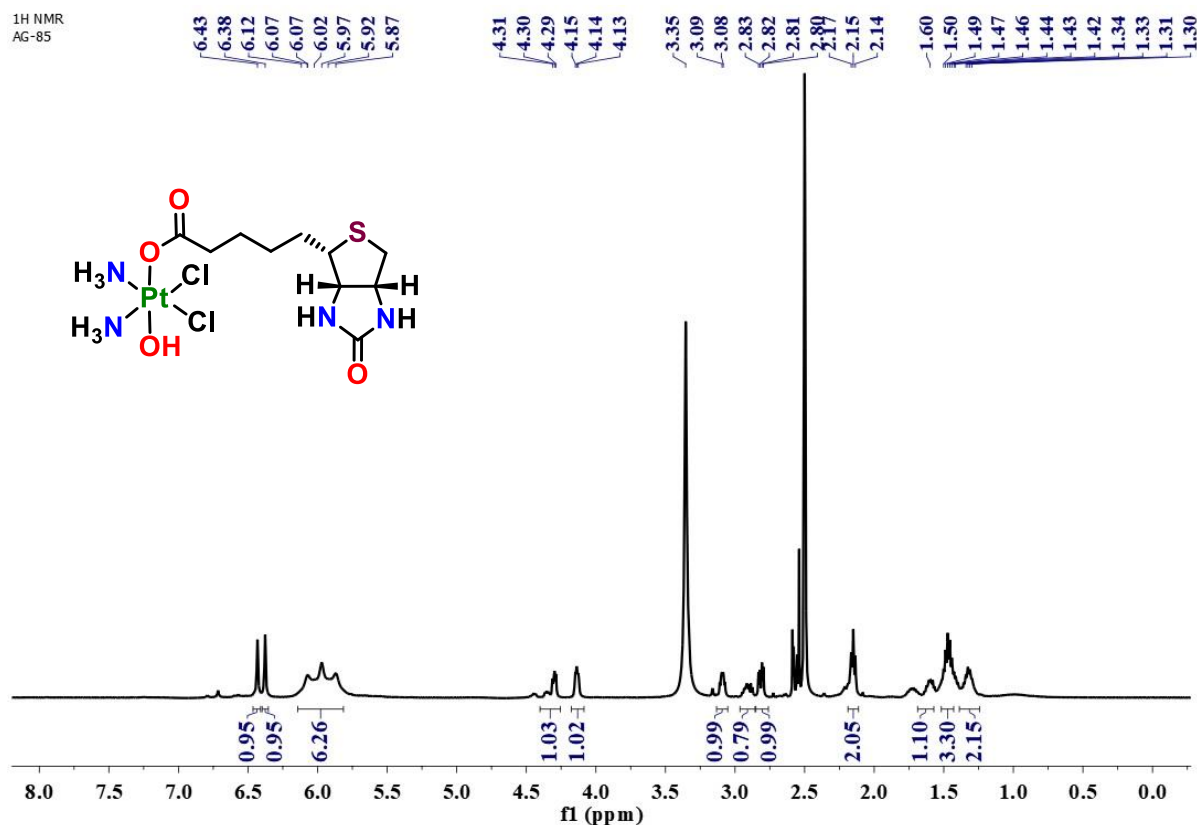


Fig. S2  $^1\text{H-NMR}$  spectrum of Pt(IV)-Biotin in DMSO- $\text{d}_6$  at 298K.

<sup>13</sup>C NMR  
AG-85 13C,

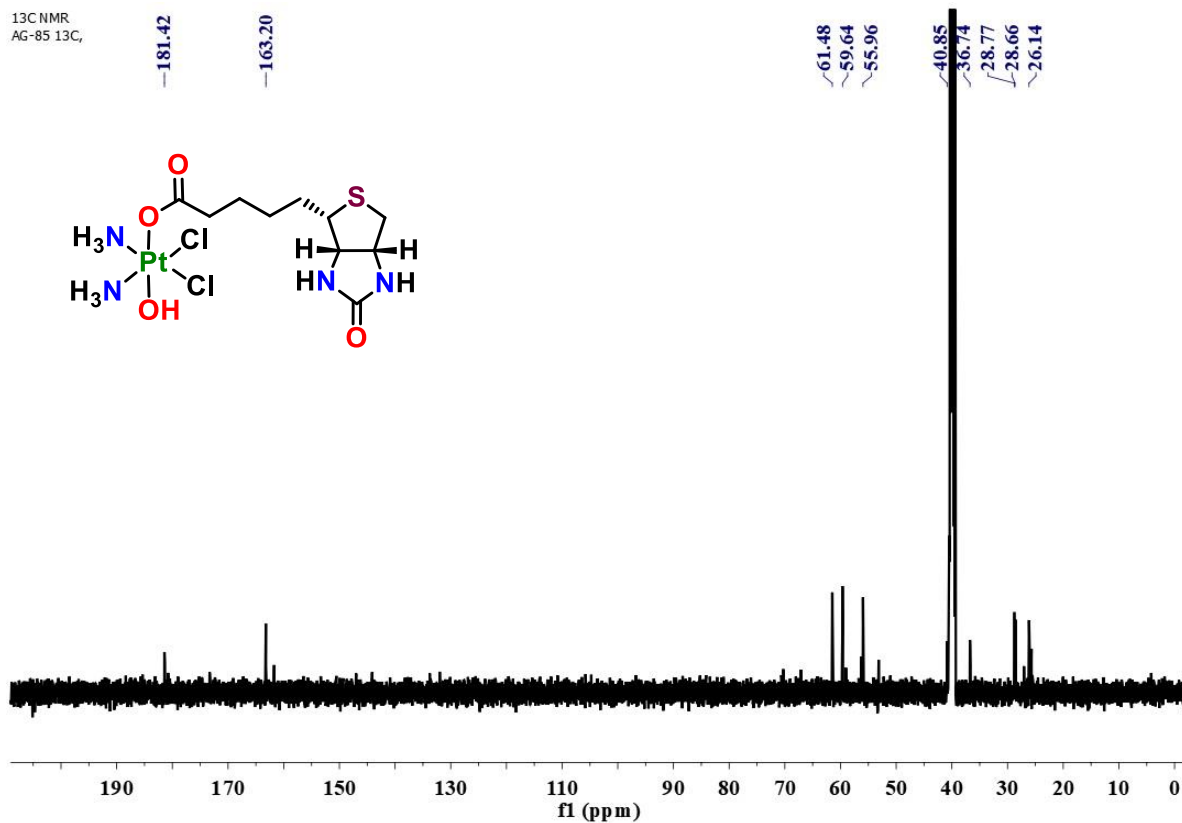


Fig. S3 <sup>13</sup>C-NMR spectrum of Pt(IV)-Biotin in DMSO-d<sub>6</sub> at 298K.

<sup>1</sup>H NMR  
AG-61 CDCl<sub>3</sub>

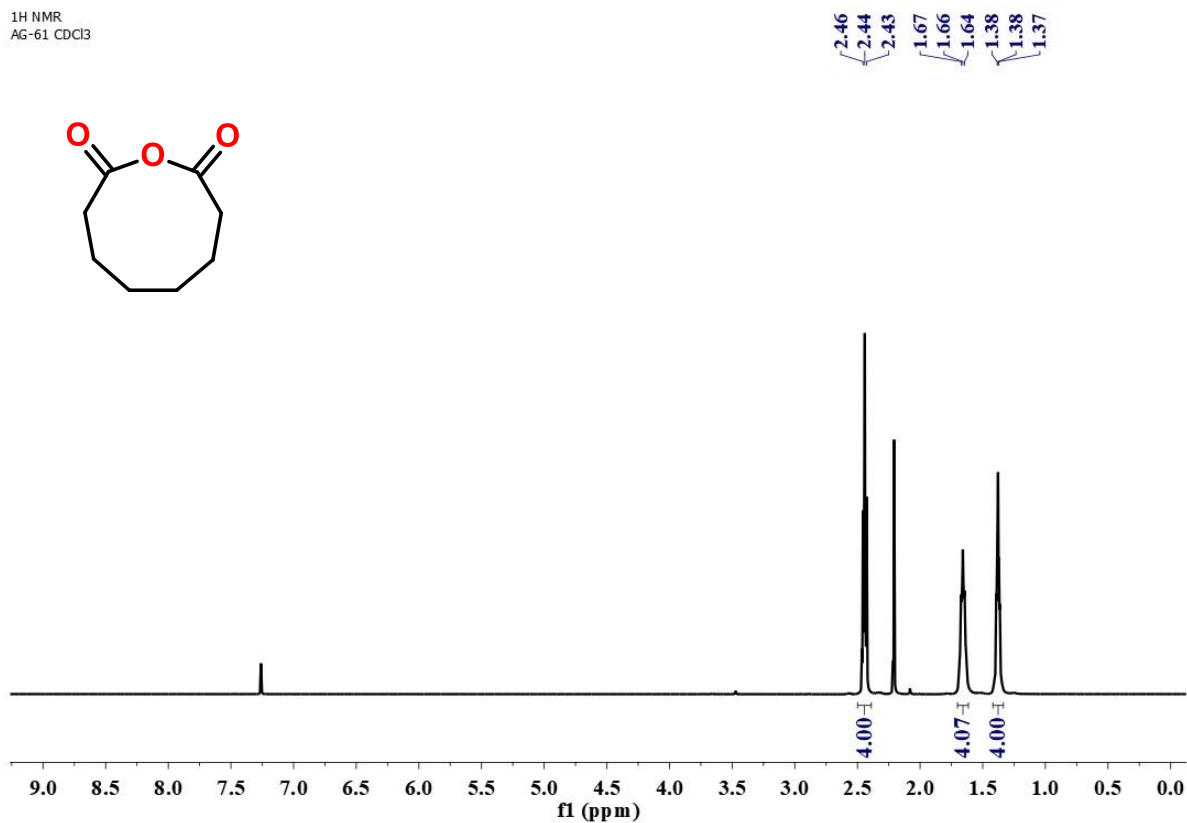


Fig. S4 <sup>1</sup>H-NMR spectrum of suberic anhydride in CDCl<sub>3</sub> at 298K.

<sup>13</sup>C NMR  
AG-61 13C

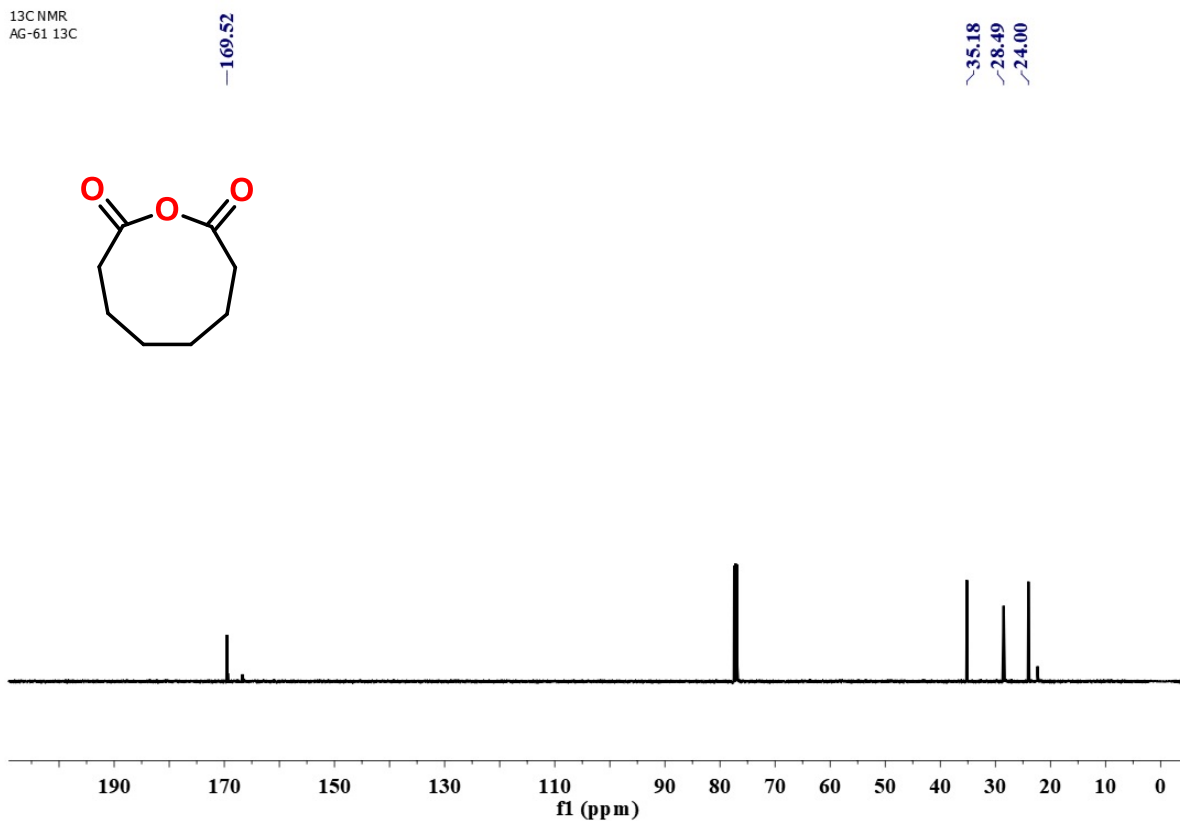


Fig. S5 <sup>13</sup>C-NMR spectrum of suberic anhydride in CDCl<sub>3</sub> at 298K.

<sup>1</sup>H NMR  
AG-63 (2)

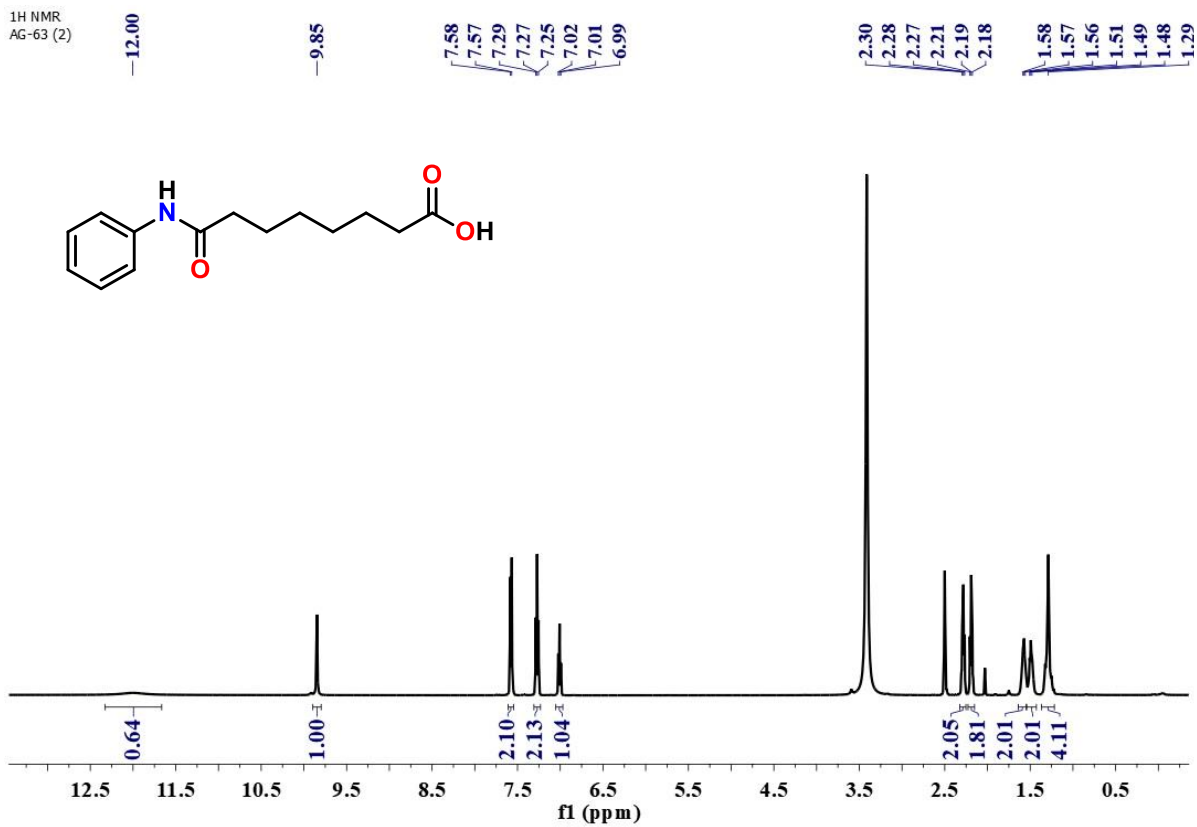


Fig. S6 <sup>1</sup>H-NMR spectrum of suberanilic acid in DMSO-d<sub>6</sub> at 298K.

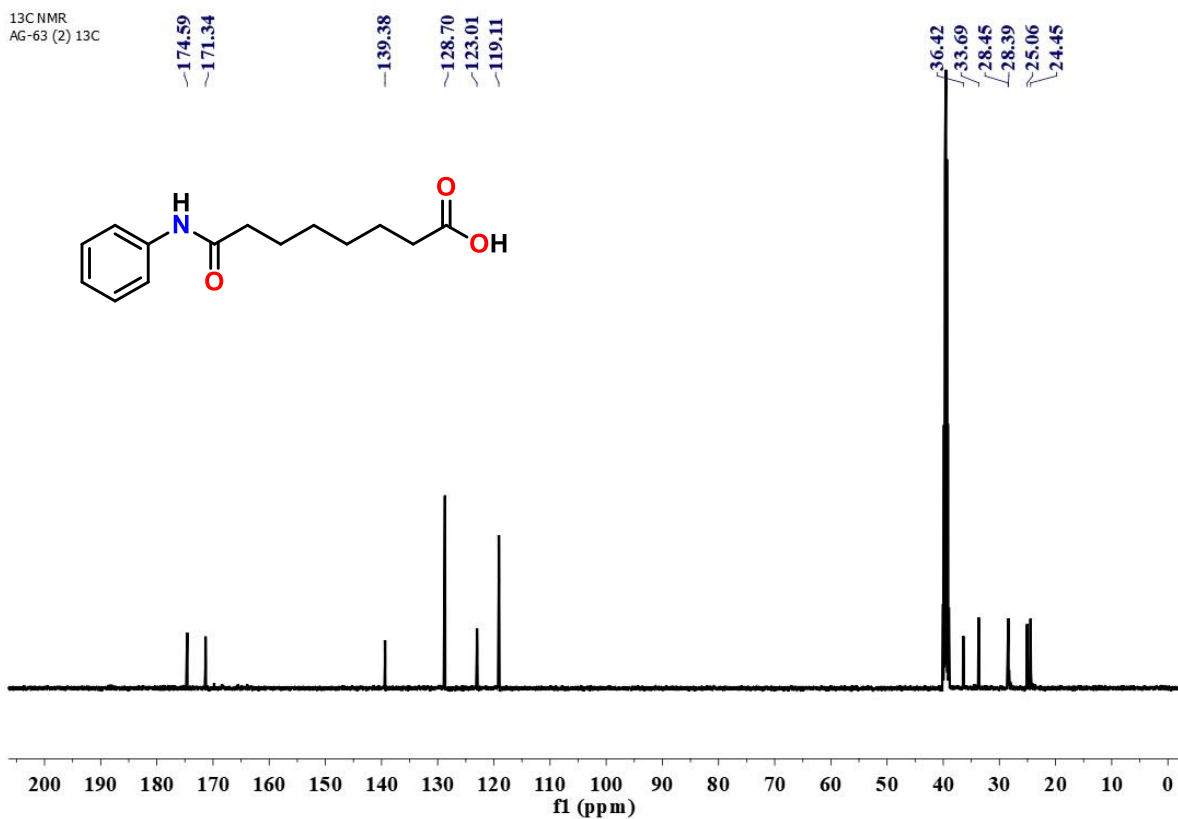


Fig. S7 <sup>13</sup>C-NMR spectrum of suberanilic acid in DMSO-d<sub>6</sub> at 298K.

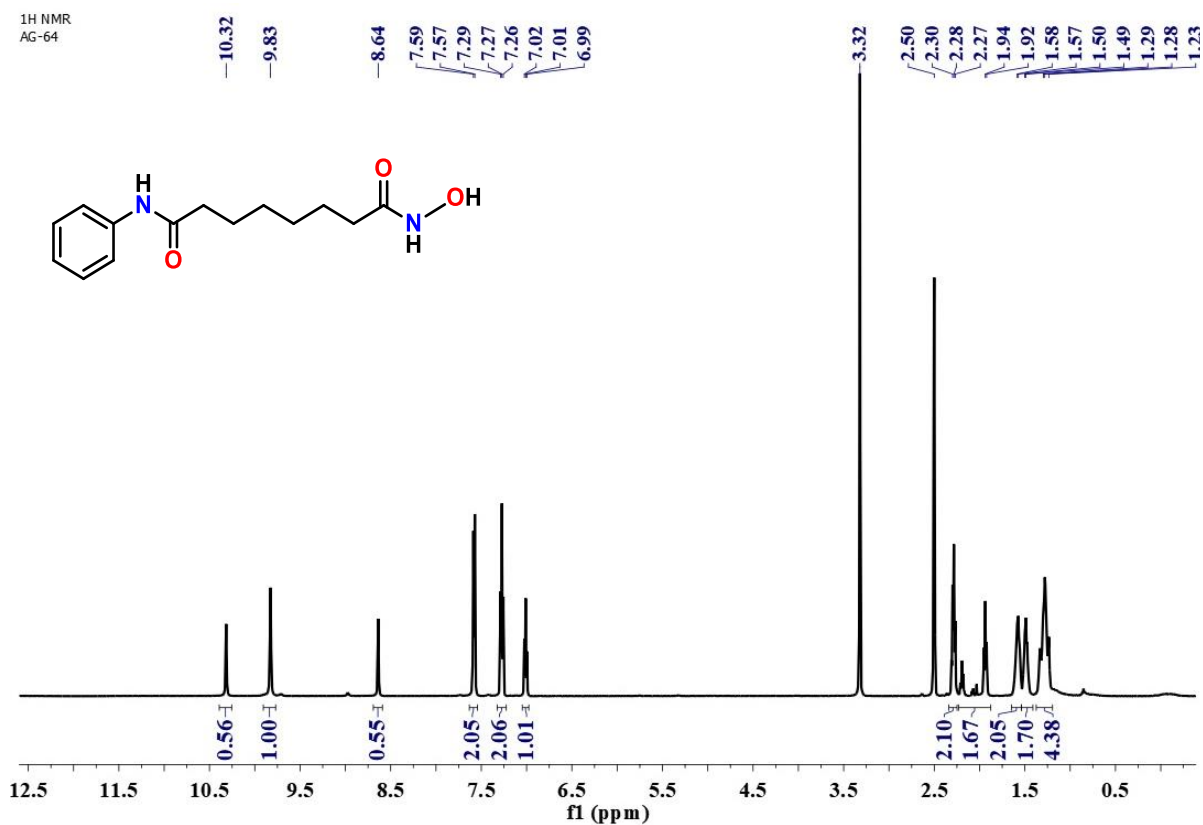


Fig. S8 <sup>1</sup>H-NMR spectrum of SAHA in DMSO-d<sub>6</sub> at 298K.

AG-156

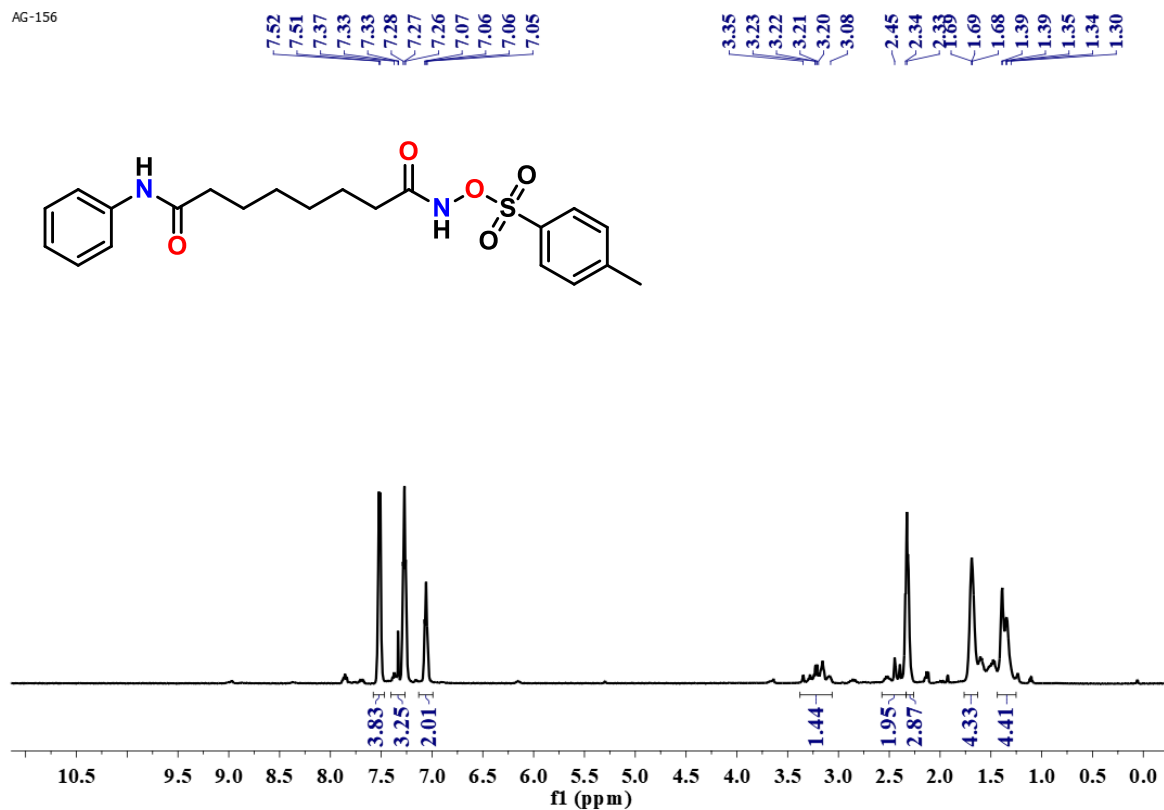


Fig. S9  $^{13}\text{C}$ -NMR spectrum of SAHA-OTs in DMSO- $d_6$  at 298K.

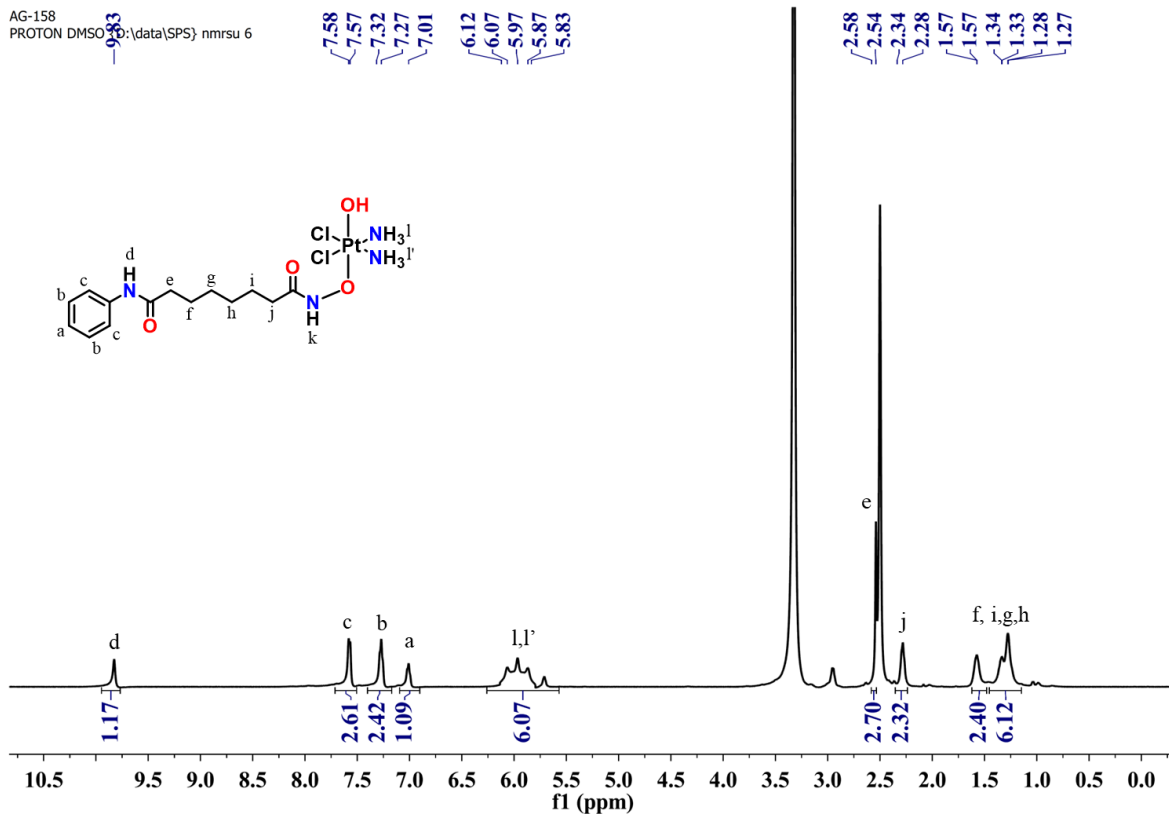
AG-158  
PROTON DMSO- $d_6$ : \data\SPS\ nmrsu 6

Fig. S10  $^1\text{H}$ -NMR spectrum of Pt(IV)-SAHA in DMSO- $d_6$  at 298K.



May22-2023  
AG-158  
C13CPD DMSO {D:\data\SPS\

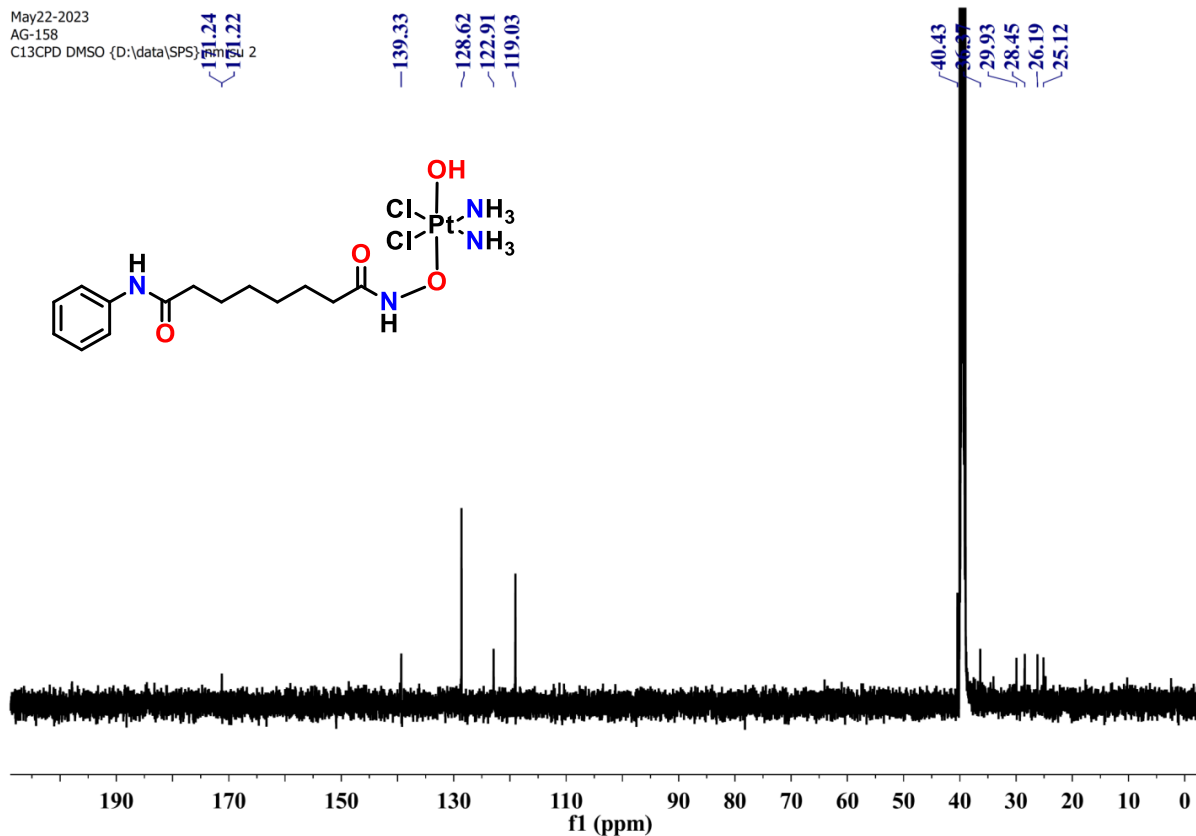


Fig. S11  $^{13}\text{C}$ -NMR spectrum of Pt(IV)-SAHA in DMSO- $d_6$  at 298K.

AG-157

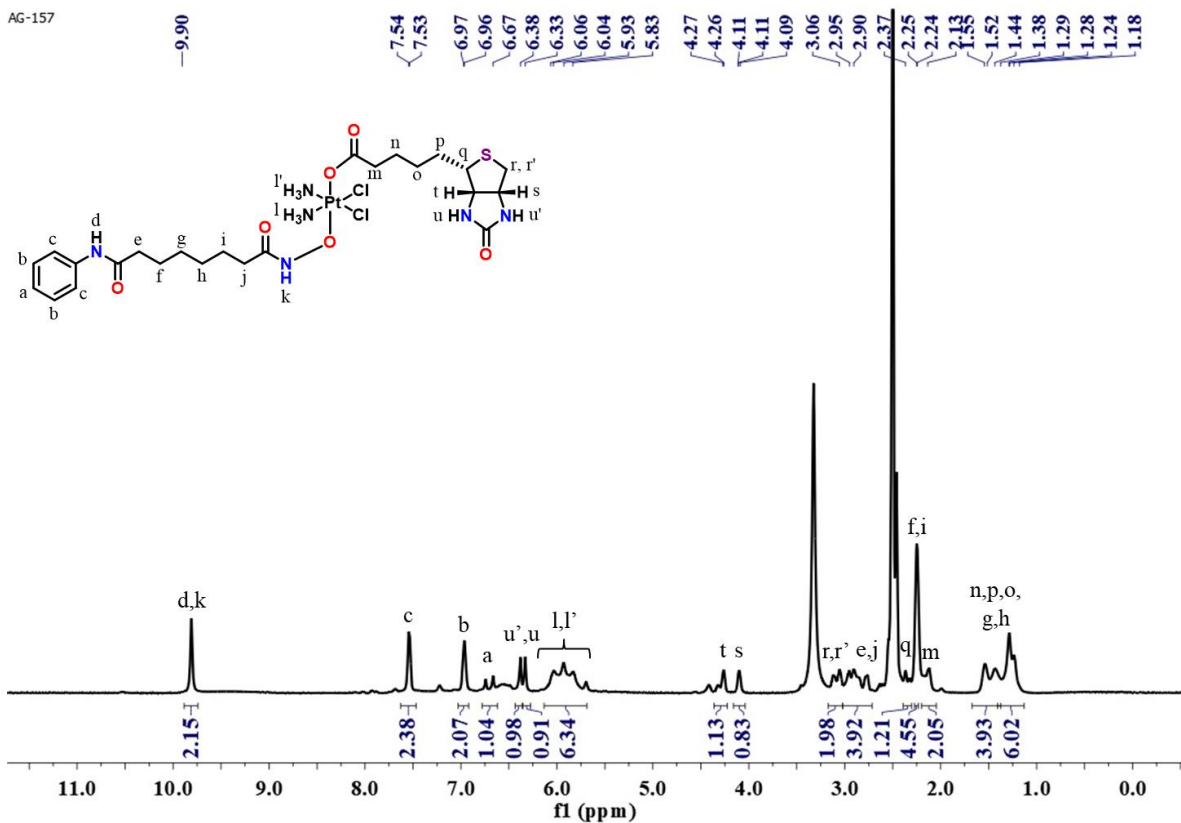


Fig. S12  $^1\text{H}$ -NMR spectrum of Biotin-Pt(IV)-SAHA in DMSO- $d_6$  at 298K.

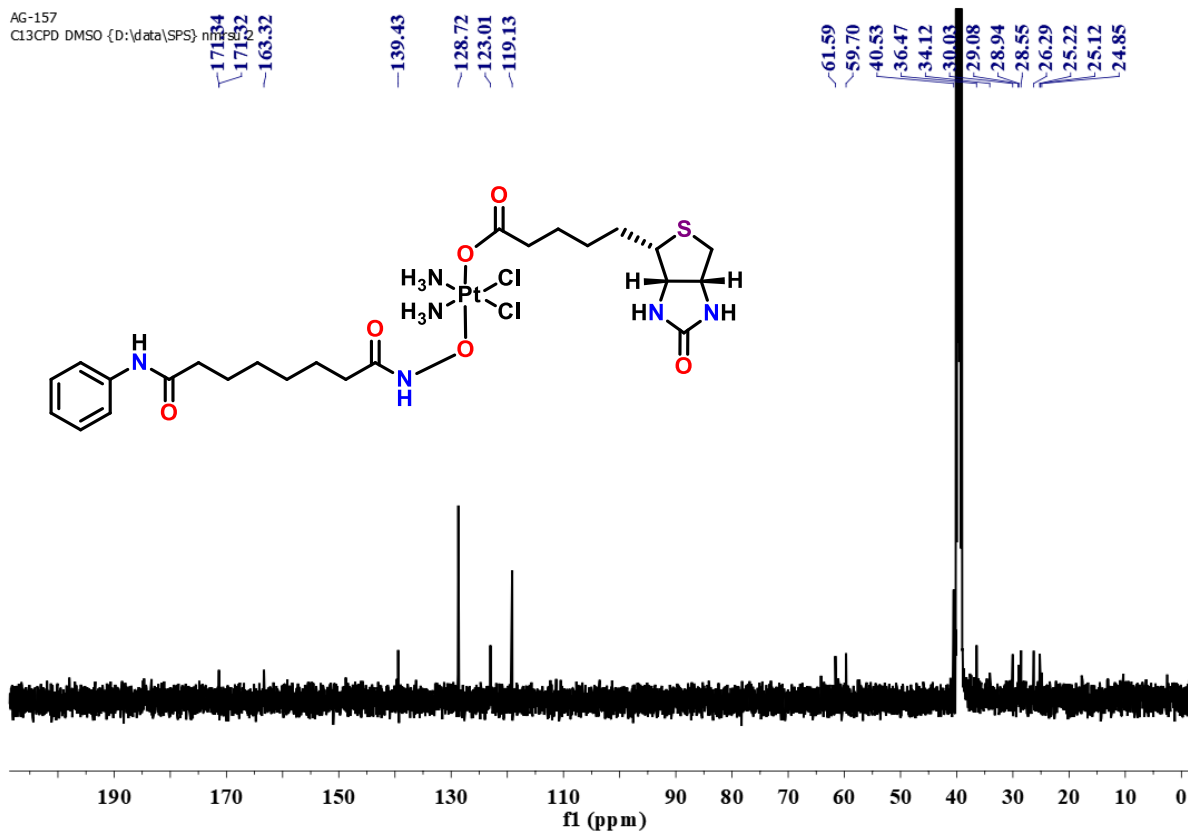


Fig. S13  $^{13}\text{C}$ -NMR spectrum of Biotin-Pt(IV)-SAHA in DMSO- $d_6$  at 298K.

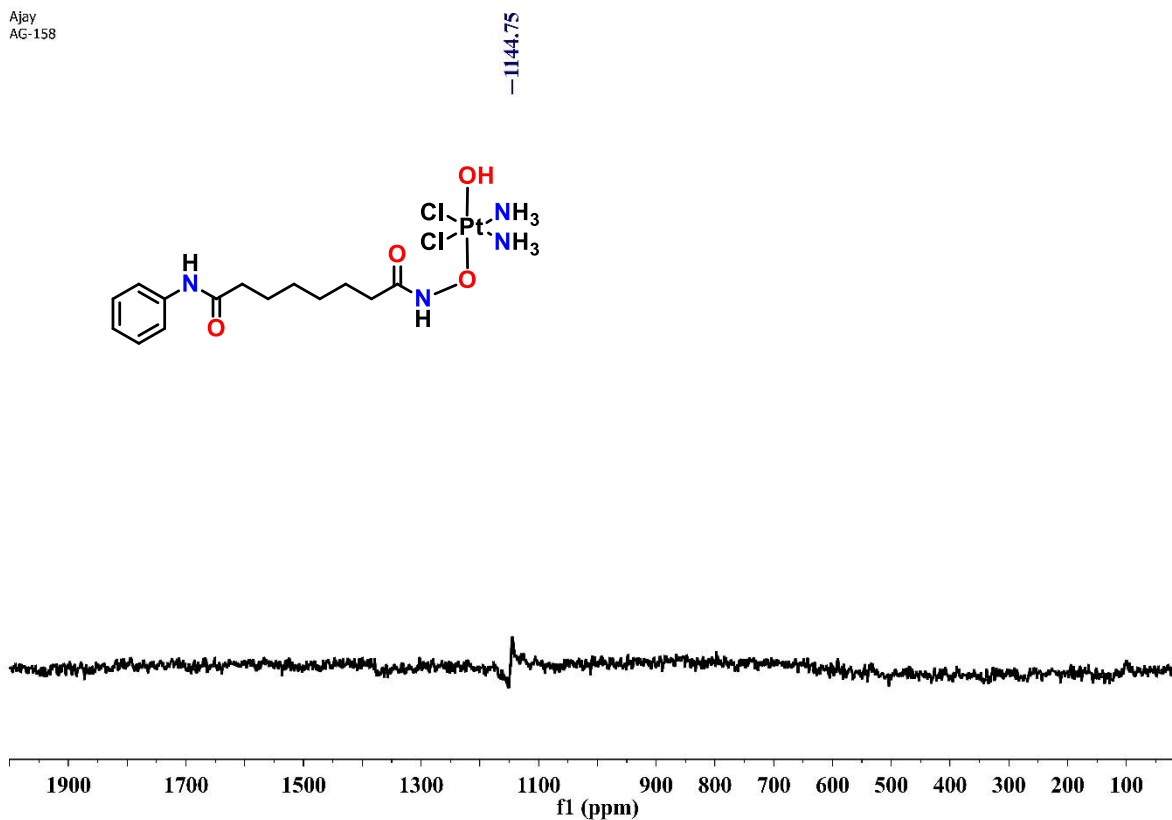
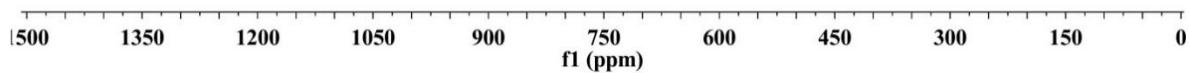
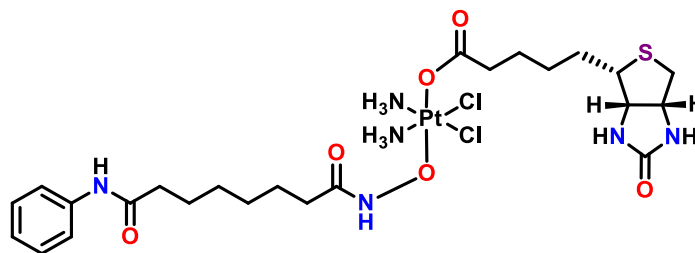


Fig. S14  $^{195}\text{Pt}$ -NMR spectrum of Pt(IV)-SAHA in DMSO- $d_6$  at 298K.

195Pt  
AG-157

—1225.97



**Fig. S15**  $^{195}\text{Pt}$ -NMR spectrum of **Biotin-Pt(IV)-SAHA** in  $\text{DMSO-d}_6$  at 298K.

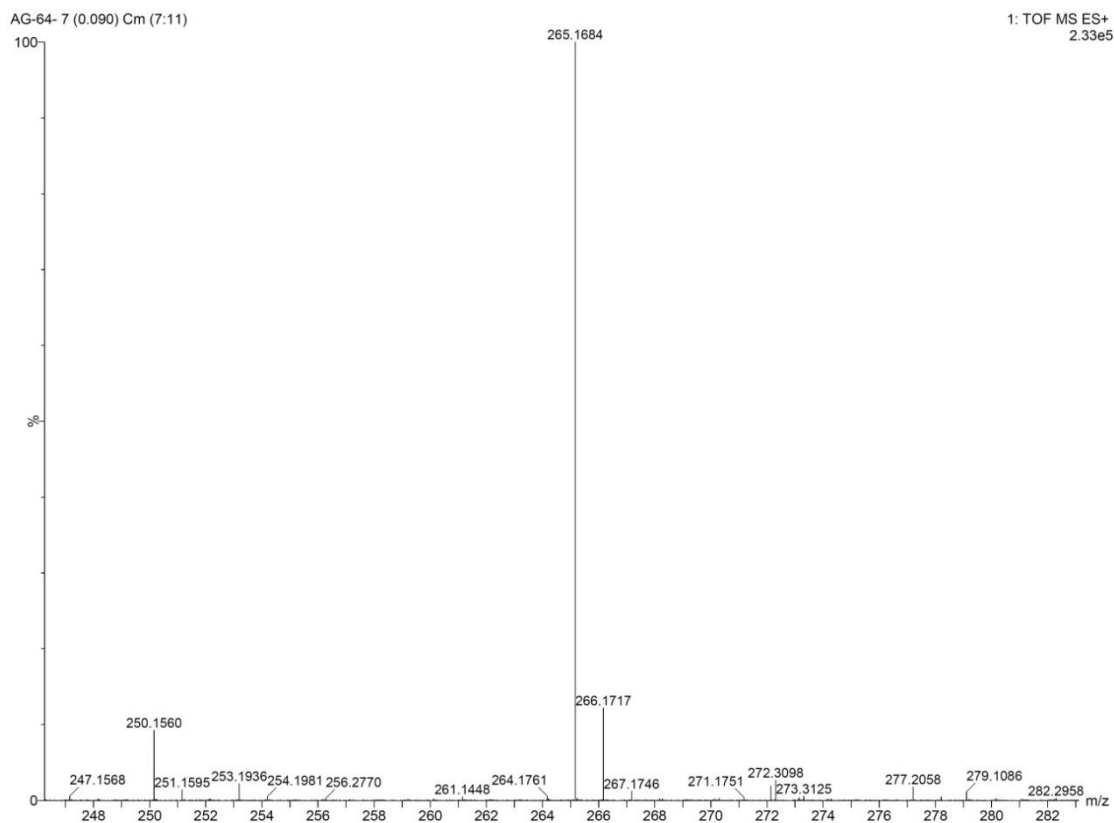


**Fig. S16** Mass spectrum of SAHA in  $\text{DCM/MeOH}$  showing the peak at 265.1684 ( $m/z$ ) assignable to  $[\text{M}+\text{H}]^+$  at 298K.

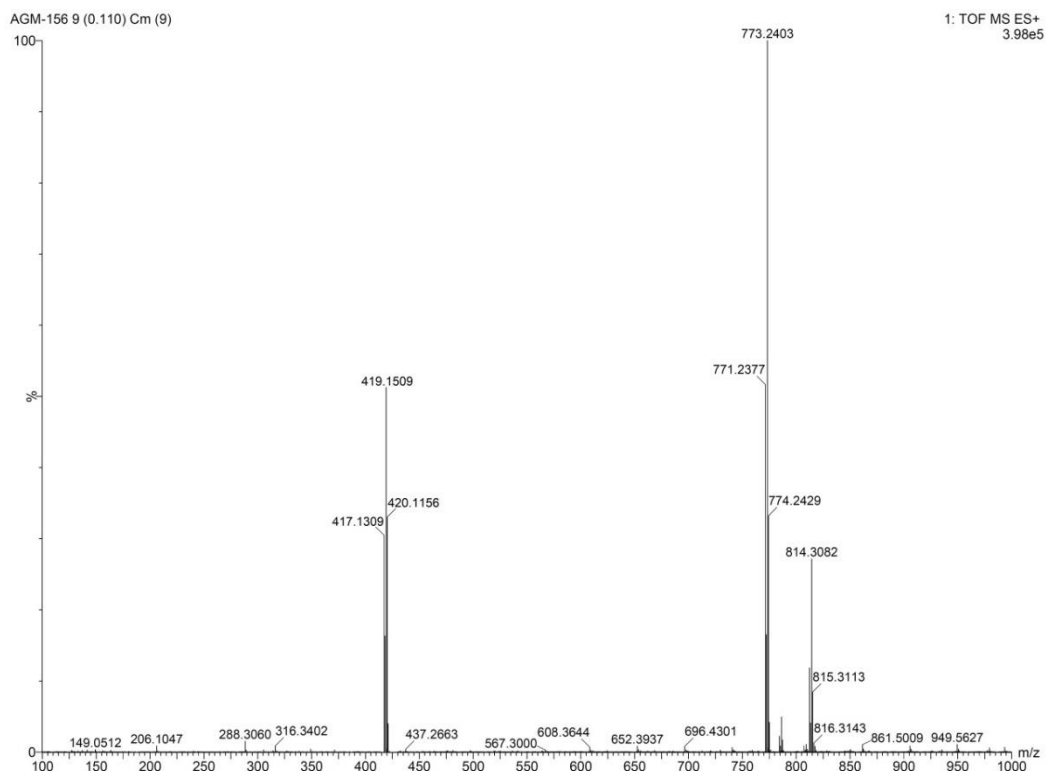


**Fig. S17** Mass spectrum of SAHA-OTs in DCM/MeOH showing the peak at 419.1509 ( $m/z$ ) assignable to  $[M+H]^+$  at 298K.

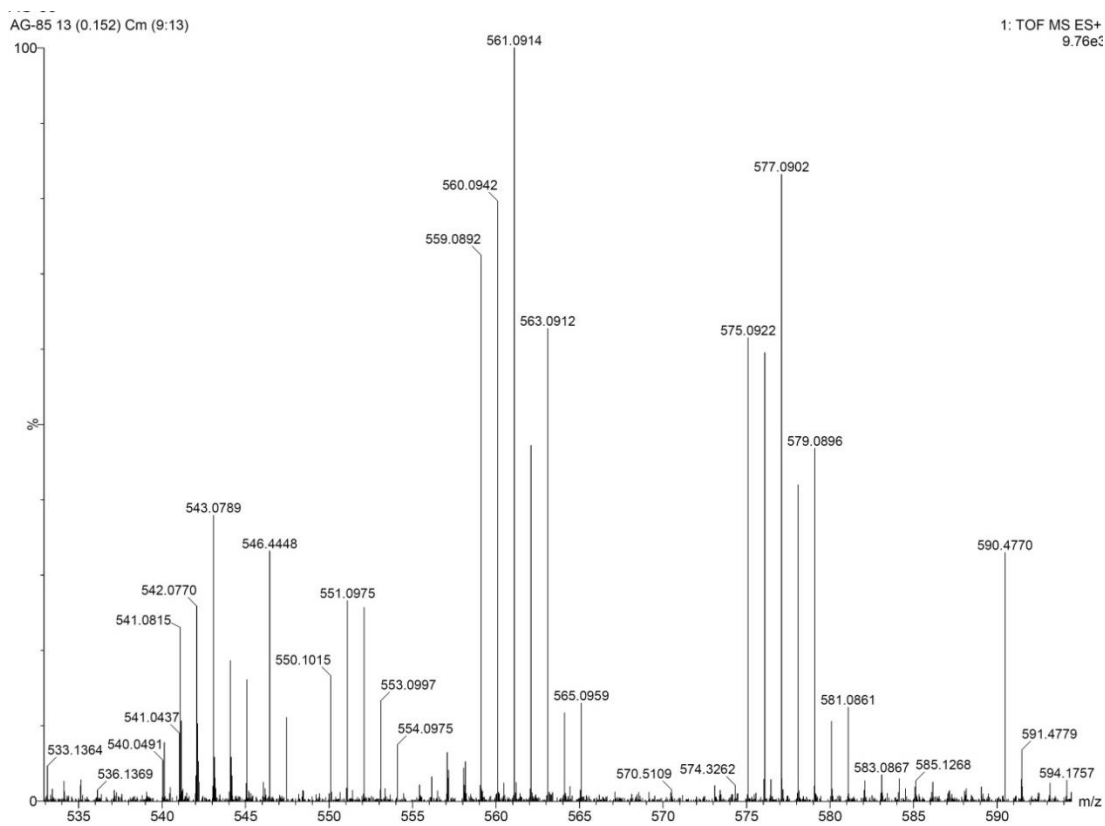


**Fig. S18** Mass spectrum of Pt(IV)-Biotin in DCM/MeOH showing the peak at 560.0942 ( $m/z$ ) assignable to  $[M+H]^+$  at 298K.

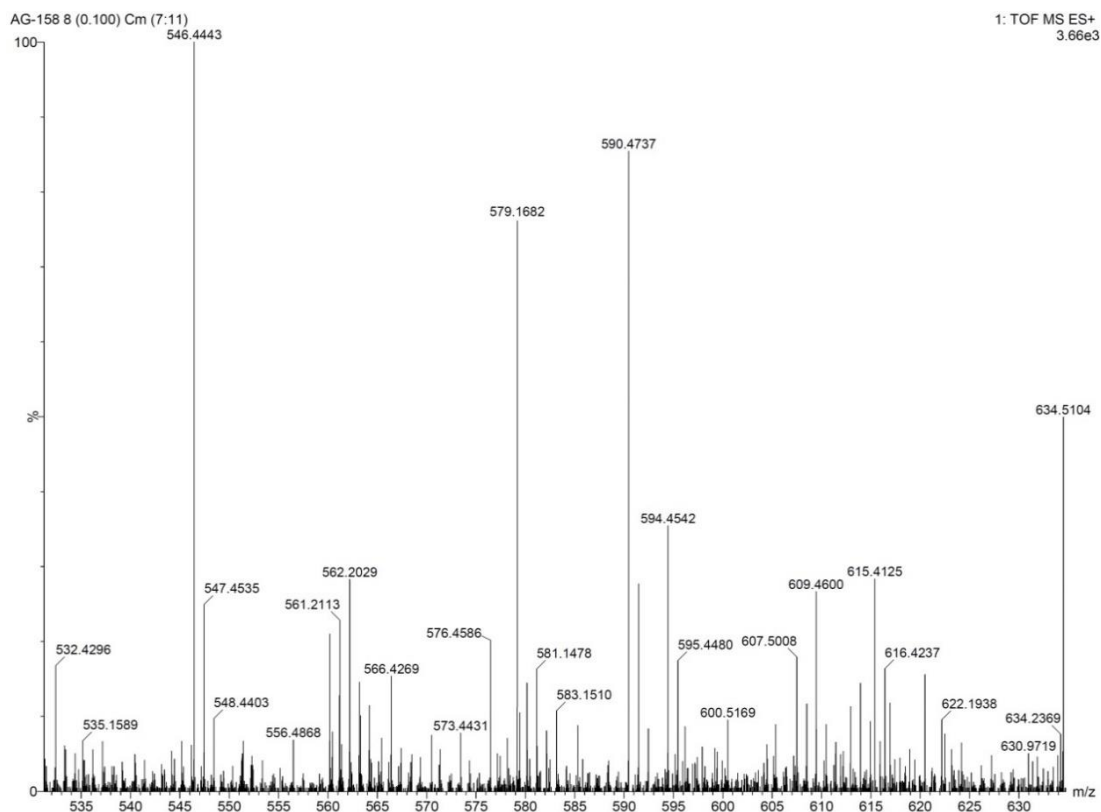


**Fig. S19** Mass spectrum of **Pt(IV)-SAHA** in DCM/MeOH showing the peak at 579.1682 ( $m/z$ ) assignable to  $[M]^+$  at 298K.

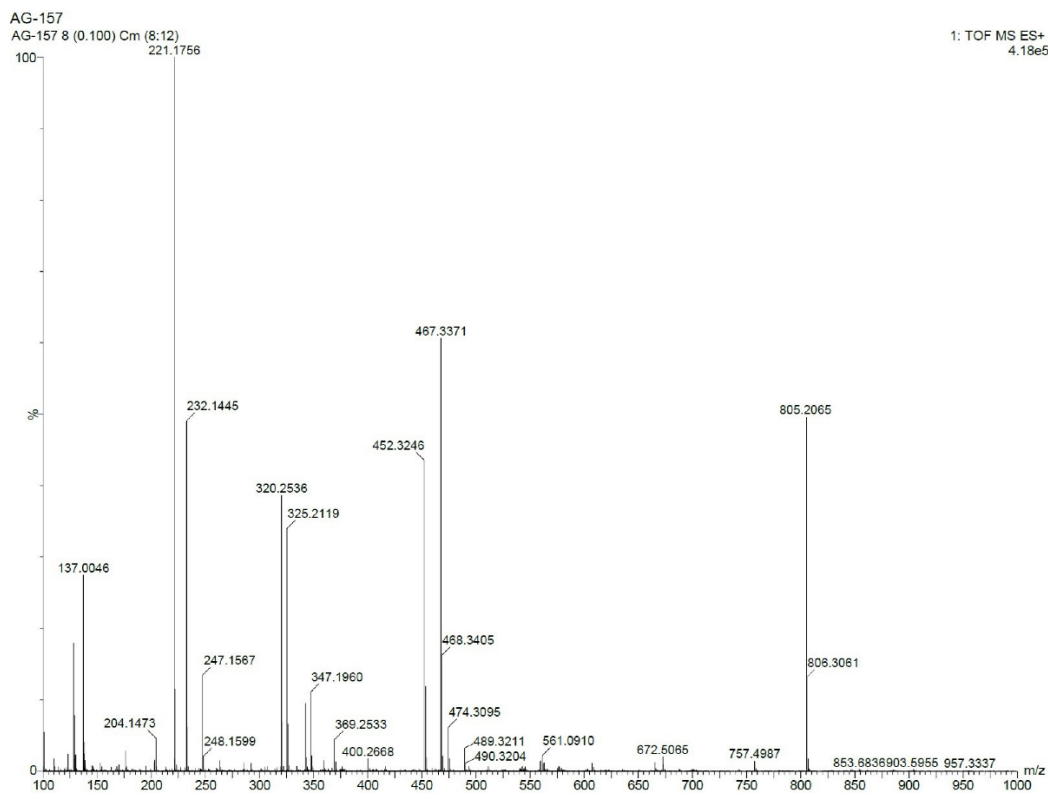


**Fig. S20** Mass spectrum of **Biotin-Pt(IV)-SAHA** in DCM/MeOH showing the peak at 805.2065 ( $m/z$ ) assignable to  $[M]^+$  at 298K.

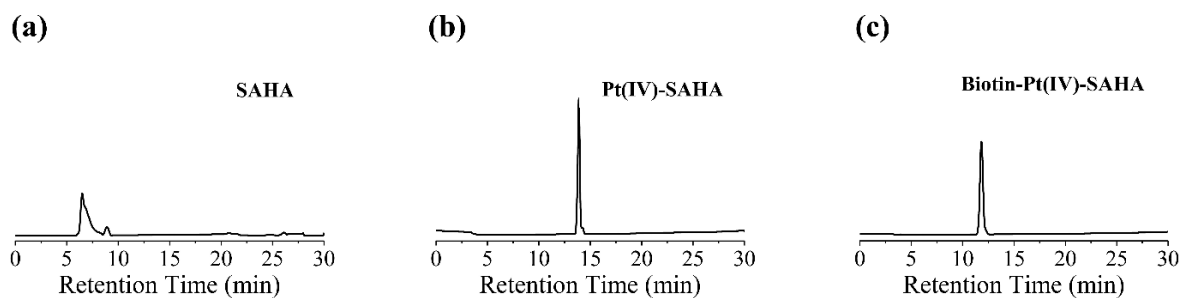


**Fig. S21** HPLC chromatograms of (a) SAHA, (b) Pt(IV)-SAHA, and (c) Biotin-Pt(IV)-SAHA are showing the purity of the compounds.

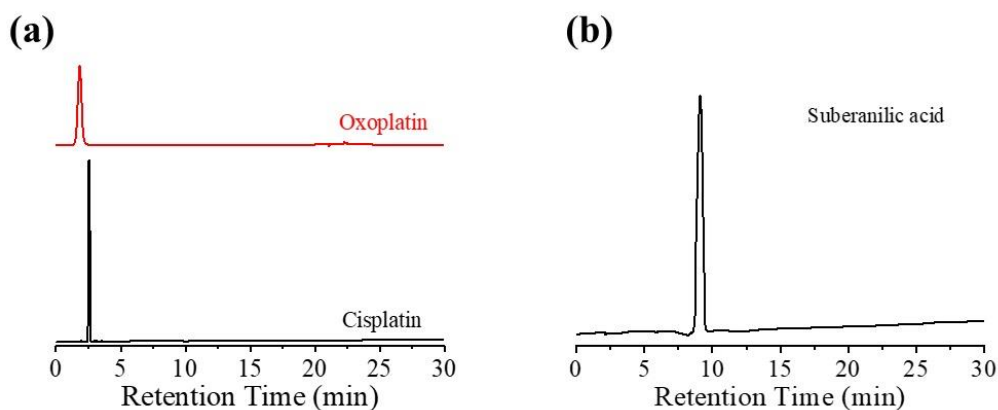


**Fig. S22** HPLC chromatograms of (a) cisplatin and oxoplatin, and (b) suberanilic acid.

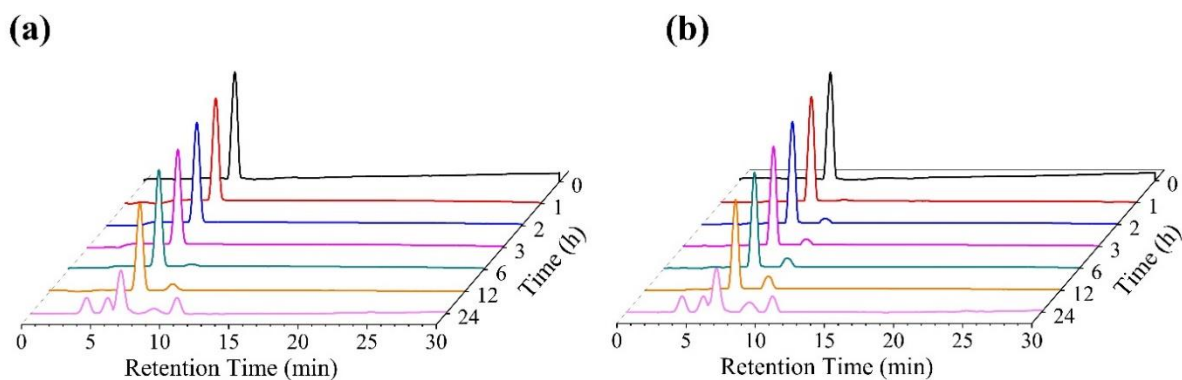


**Fig. S23** Stability of SAHA (a) in PBS (5 mM, pH 7.4) and (b) in 5 mM ascorbate monitored by HPLC.

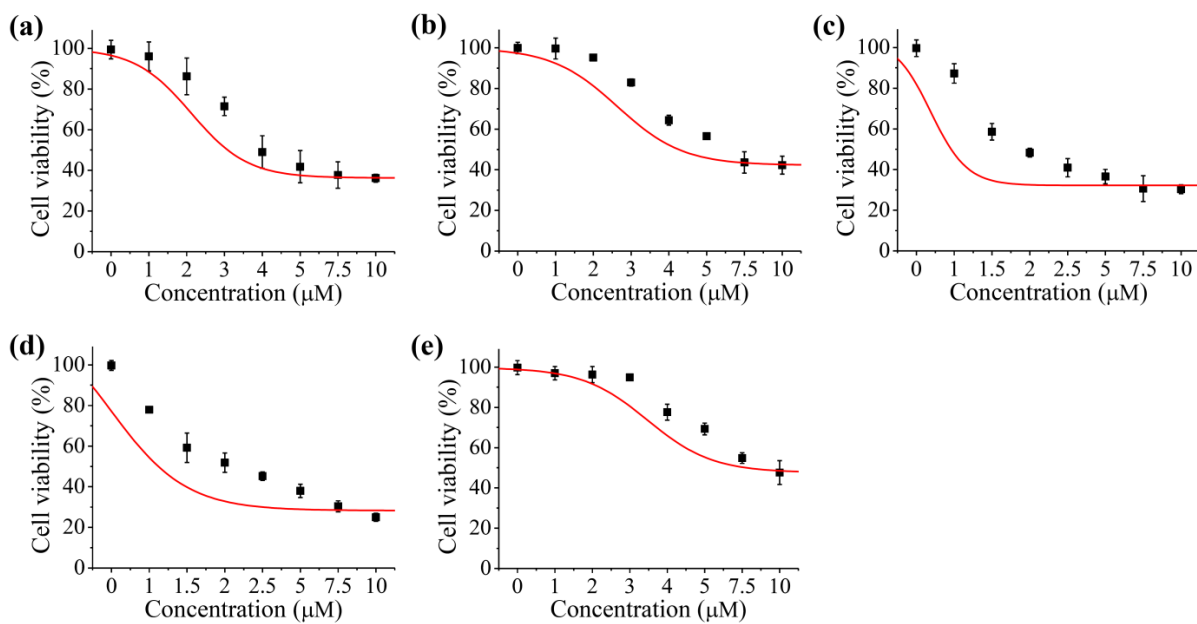


**Fig. S24** Cell viability assay in MCF7 cells treated with the (a) **Pt(IV)-Biotin**, (b) **Pt(IV)-SAHA**, (c) **Biotin-Pt(IV)-SAHA**, (d) SAHA, and (e) cisplatin after 72 h incubation.

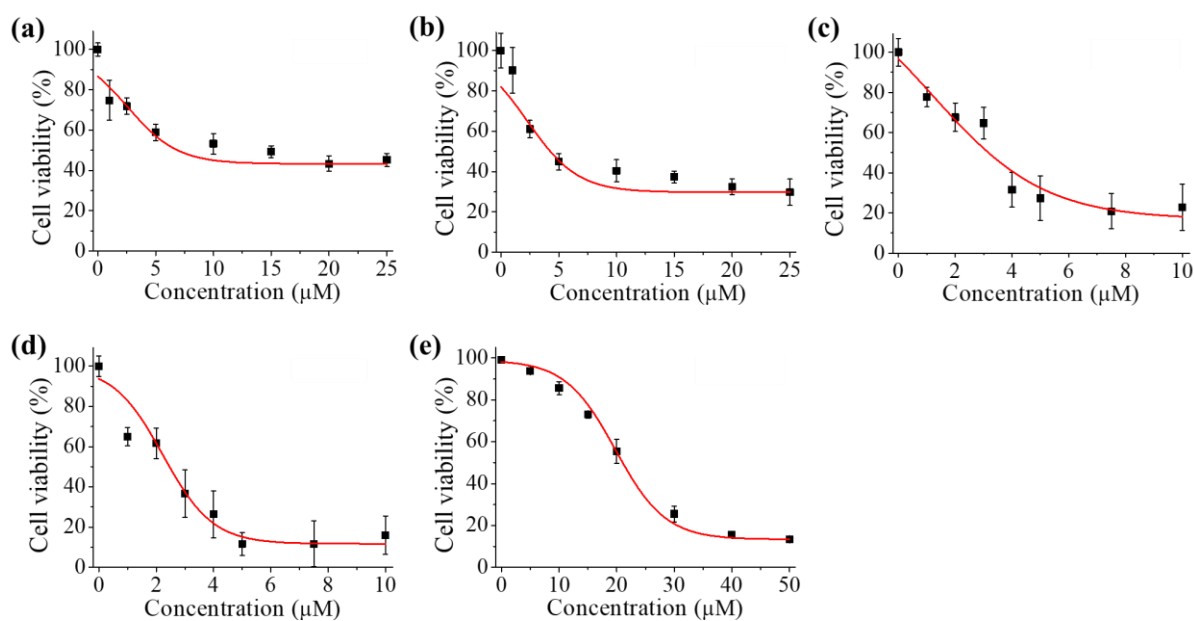


**Fig. S25** Cell viability assay in A549 cells treated with the (a) **Pt(IV)-Biotin**, (b) **Pt(IV)-SAHA**, (c) **Biotin-Pt(IV)-SAHA**, (d) SAHA, and (e) cisplatin after 72 h incubation.

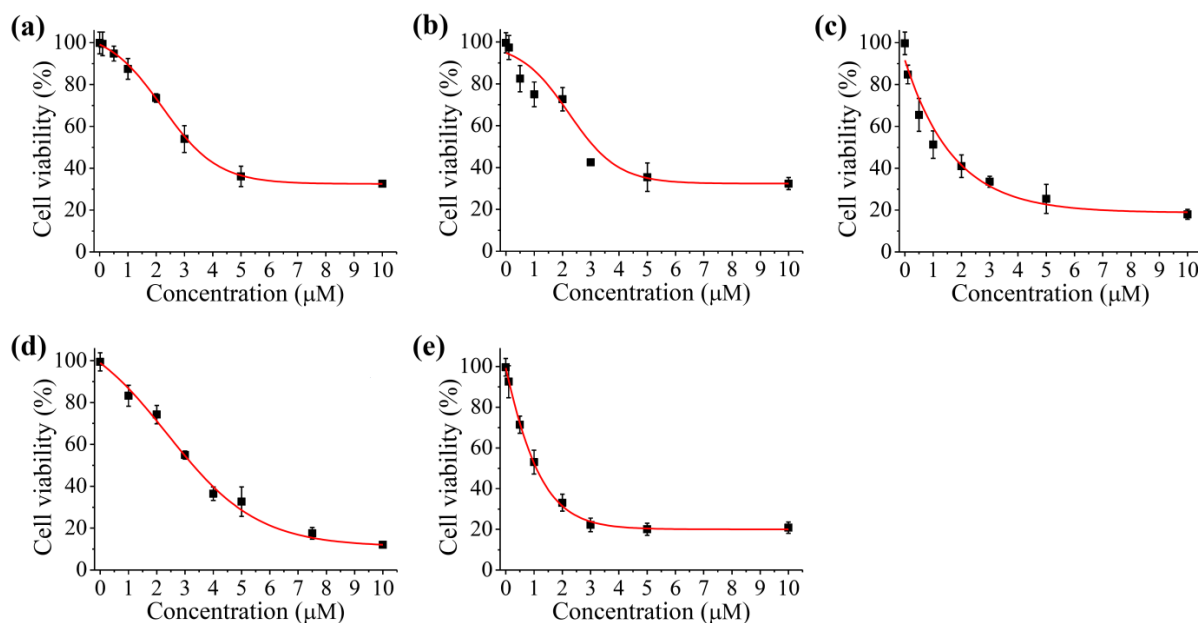


**Fig. S26** Cell viability assay in A2780 cells treated with the (a) **Pt(IV)-Biotin**, (b) **Pt(IV)-SAHA**, (c) **Biotin-Pt(IV)-SAHA**, (d) SAHA, and (e) cisplatin after 72 h incubation.

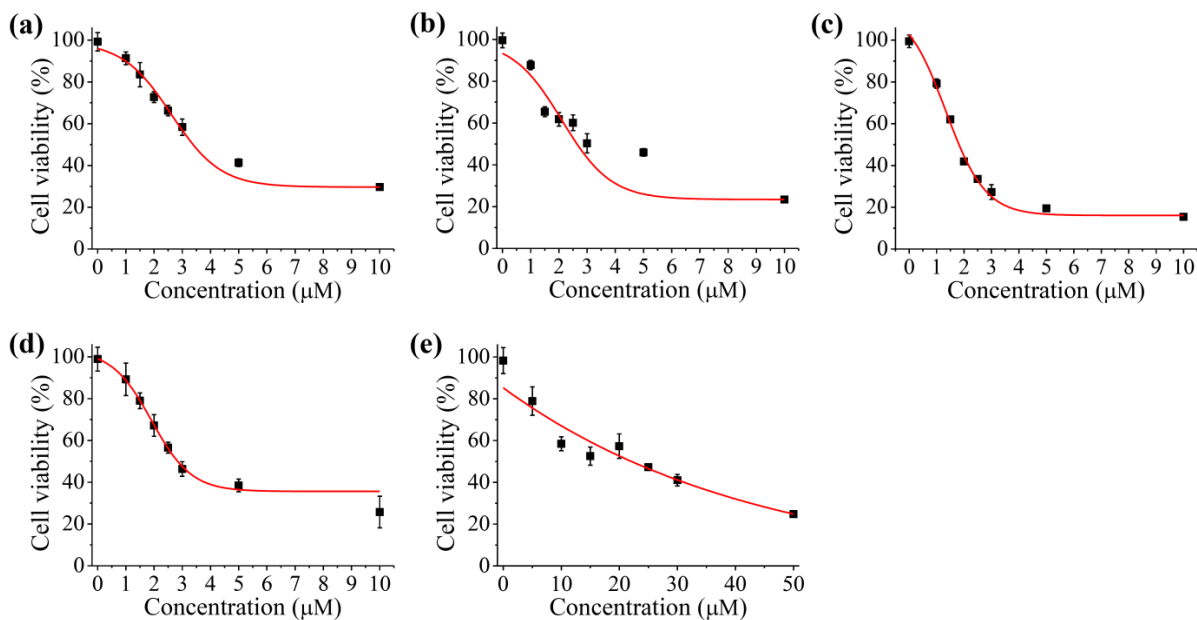


**Fig. S27** Cell viability assay in A2780cisR cells treated with the (a) **Pt(IV)-Biotin**, (b) **Pt(IV)-SAHA**, (c) **Biotin-Pt(IV)-SAHA**, (d) SAHA, and (e) cisplatin after 72 h incubation.



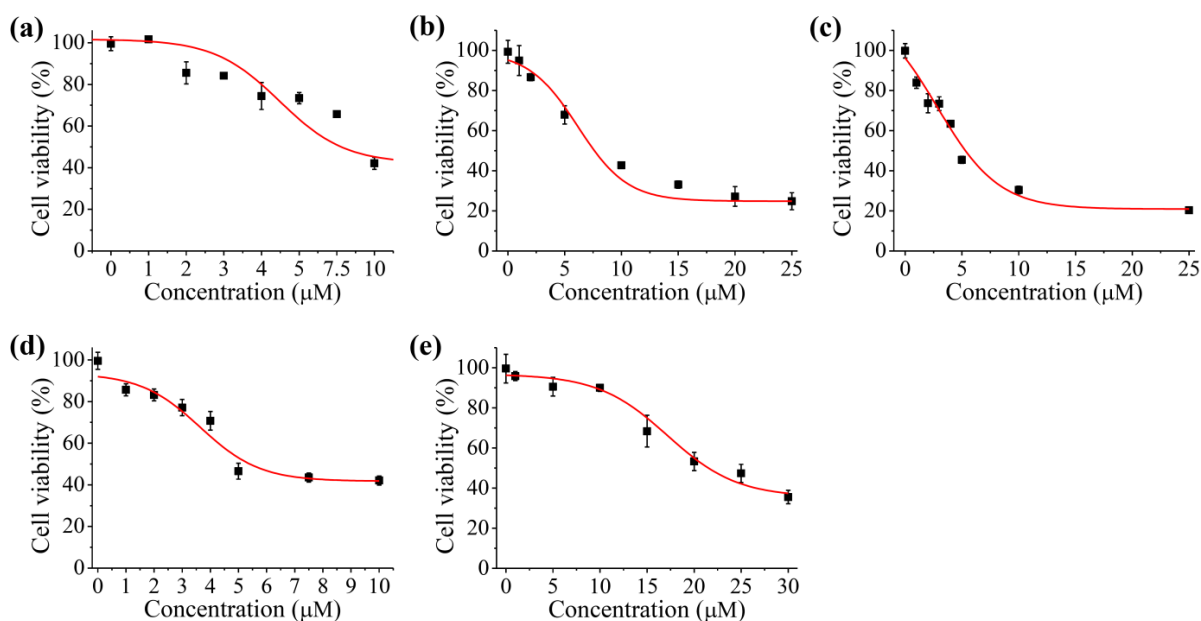


**Fig. S28** Cell viability assay in HEK293 cells treated with the (a) **Pt(IV)-Biotin**, (b) **Pt(IV)-SAHA**, (c) **Biotin-Pt(IV)-SAHA**, (d) SAHA, and (e) cisplatin after 72 h incubation.

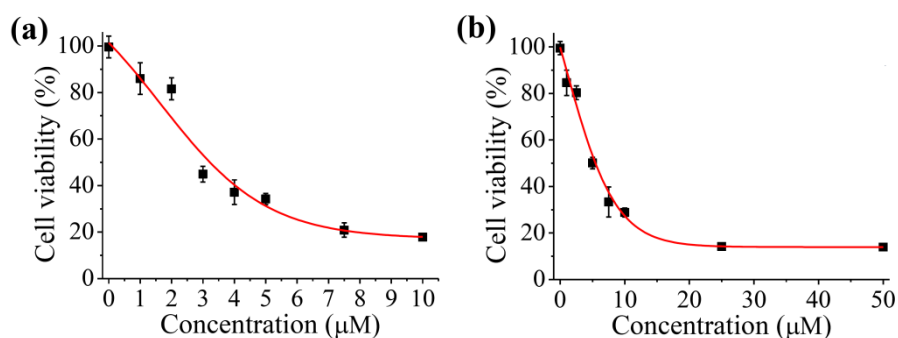


**Fig. S29** Cell viability assay in A2780 cells treated with the (a) **Pt(IV)-Biotin + SAHA** at their equimolar concentration and (b) **cisplatin + SAHA** after 72 h incubation.

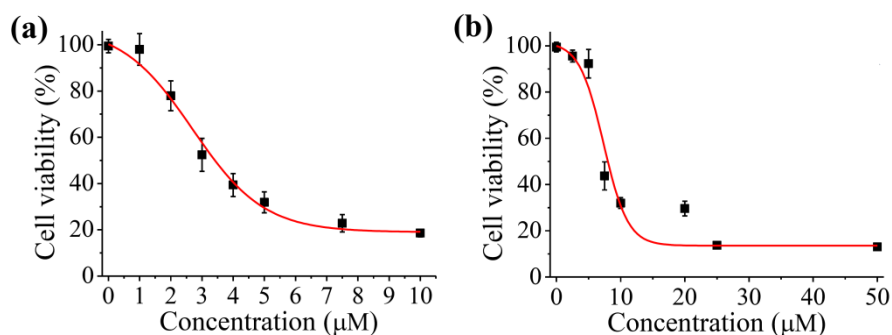


**Fig. S30** Cell viability assay in A2780cisR cells treated with the (a) **Pt(IV)-Biotin + SAHA** at their equimolar concentration (b) **cisplatin + SAHA** after 72 h incubation.

## References

1. A. Gupta, A. K. Pandey, T. Mondal, J. Bhattacharya and P. K. Sasmal, Multifunctional Iridium(III)-Platinum(IV) Conjugates as Potent Anticancer Theranostic Agents, *J. Med. Chem.*, 2023, **66**, 8687–8704.
2. G. Kumari, A. Gupta, R. K. Sah, A. Gautam, M. Saini, A. Gupta, A. K. Kushawaha, S. Singh and P. K. Sasmal, Development of Mitochondria Targeting AIE-Active Cyclometalated Iridium Complexes as Potent Antimalarial Agents, *Adv. Healthcare Mater.*, 2023, **12**, 2202411.